Japanese patients with mitochondrial 3-hydroxy-3-methylglutaryl-CoA synthase deficiency: *In vitro* functional analysis of five novel *HMGCS2* mutations

YASUHIKO AGO[1], HIROKI OTSUKA[1], HIDEO SASAI[1,2], ELSAYED ABDELKREEM[3], MINA NAKAMA[1,2], YUKA AOYAMA[4], HIDEKI MATSUMOTO[1], RYOJI FUJIKI[5], OSAMU OHARA[5], KAZUMASA AKIYAMA[6], KAORI FUKUI[7], YORIKO WATANABE[7,8], YOKO NAKAJIMA[9], HIDENORI OHNISHI[1], TETSUYA ITO[9] and TOSHIYUKI FUKAO[1,2*]

[1]Department of Pediatrics, Graduate School of Medicine; [2]Clinical Genetics Center, Gifu University Hospital, Gifu, Gifu 501-1194, Japan; [3]Department of Pediatrics, Faculty of Medicine, Sohag University, Sohag 82524, Egypt; [4]Department of Biomedical Sciences, College of Life and Health Sciences, Education and Training Center of Medical Technology, Chubu University, Kasugai, Aichi 487-8501; [5]Department of Applied Genomics, Kazusa DNA Research Institute, Kisarazu, Chiba 292-0818; [6]Akiyama Children's Clinic, Kitami, Hokkaido 090-0051; [7]Department of Pediatrics and Child Health; [8]Research Institute of Medical Mass Spectrometry, Kurume University School of Medicine, Kurume, Fukuoka 830-0011; [9]Department of Pediatrics, Fujita Health University School of Medicine, Toyoake, Aichi 470-1192, Japan

Received December 11, 2019; Accepted June 17, 2020

DOI: 10.3892/etm.2020.9166

Abstract. Mitochondrial 3-hydroxy-3-methylglutaryl-CoA synthase (HMGCS2) deficiency is a metabolic disorder caused by mutations in the *HMGCS2* gene. The present study describes the identification of four cases of HMGCS2 deficiency in Japan. Hepatomegaly and severe metabolic acidosis were observed in all cases. Fatty liver was identified in three cases, which suggested the unavailability of fatty acids. All patients presented with a high C2/C0 ratio, suggesting that the fatty acid oxidation pathway was normal during metabolic crisis. Genetic analyses revealed five rare, novel variants (p.G219E, p.M235T, p.V253A, p.S392L and p.R500C) in *HMGCS2*. To confirm their pathogenicity, a eukaryotic expression system and a bacterial expression system was adopted that was successfully used to obtain affinity-purified HMGCS2 protein with measurable activity. Purified M235T, S392L and R500C proteins did not retain any residual activity, whilst the V253A variant showed some residual enzymatic activity. Judging from the transient expression experiment in 293T cells, the G219E variant appeared to be unstable. In conclusion, the present study identified five novel variants of *HMGCS2* that were indicated to be pathogenic in four patients affected by *HMGCS2* deficiency.

Correspondence to: Dr Hidenori Ohnishi, Department of Pediatrics, Graduate School of Medicine, Gifu University Hospital, 1-1 Yanagido, Gifu, Gifu 501-1194, Japan
E-mail: ohnishih@gifu-u.ac.jp

*Deceased

Key words: bacterial expression system, C2/C0, disease-causing mutation, functional analysis, mitochondrial 3-hydroxy-3-methylglutaryl-CoA synthase

Introduction

Ketone bodies, which are mainly generated from fatty acids, are important alternative energy sources during fasting (1,2). Mitochondrial 3-hydroxy-3-methylglutaryl-CoA synthase (HMGCS2; Nomenclature Committee of the International Union of Biochemistry and Molecular Biology classification no. EC 2.3.3.10) catalyzes the condensation of acetoacetyl-CoA and acetyl-CoA to form 3-hydroxy-3-methylglutaryl-CoA (HMG-CoA), which is the rate-limiting step of ketone body synthesis (3,4).

HMGCS2 deficiency (Online Mendelian Inheritance in Man reference no. 605911) is a metabolic disorder caused by mutations in the *HMGCS2* gene, which consists of 10 exons located on chromosome 1p12-13 (5). To date, nearly 30 cases that have been reported in the literature describe an autosomal recessive inheritance pattern (6). Most patients present with symptomatic hypoketotic hypoglycemia and hepatomegaly after a period of prolonged fasting or intercurrent illness (6). Metabolic acidosis is often noted during the acute phase (7-12). During the metabolic crisis, the serum concentration of free fatty acids (FFAs) is relatively high when compared with that of the total ketone bodies (TKBs) (6). The clinical presentation is similar to that observed with fatty acid β-oxidation defects, but the urinary organic acids and blood acylcarnitine profiles are non-specific in cases of HMGCS2 deficiency. Urinary

4-hydroxy-6-methyl-2-pyrone (4HMP) is a possible specific marker of the disorder (10). While the use of liver samples for an enzyme assay or immunoblotting aids in diagnosis (13), obtaining these samples is an invasive procedure. The diagnosis of HMGCS2 deficiency is therefore usually based on genetic analysis.

Genetic analyses were performed on several suspected cases referred to Department of Pediatrics, Graduate School of Medicine, Gifu-University (Gifu, Japan) from 2005. From these cases, four patients carried six rare non-synonymous variants of *HMGCS2*, among which five of the variants have, to the best of our knowledge, not been reported previously. To confirm their pathogenicity *in vitro*, the variant enzymes were expressed in 293T cells and the *Escherichia coli* strain BL21(DE3).

Materials and methods

Cases. The patients in all four cases were born to non-consanguineous Japanese parents with no family history of inherited metabolic disease. All of the patients were born uneventfully following an uncomplicated term pregnancy. Only patient 3 was a light-for-date infant; the others had normal birth weights. After birth, physical growth and neurological development until the onset of disease were normal except for in patient 4. Clinical features and the results of first blood examinations showing metabolic decompensation are listed in Table I. Before enrolling the four patients into this study, written informed consent was obtained from the parents of each patient by their attending pediatrician. This study was approved by the Ethical Committee of the Graduate School of Medicine, Gifu University, Japan (approval no. 29-503).

On the day of symptom onset, in July 2013 (the exact day remained anonymous to protect the patient's identity), patient 1 was 8 months old. She took breast milk in the early morning. Afterward, she could not obtain sufficient nutrition orally and gradually became lethargic, before she began vomiting at 6 PM. At Nagoya City University Hospital (looked after by TI; Nagoya, Japan), she presented with tachypnea, tachycardia and hepatomegaly, prompting the first blood test. In spite of the immediate correction of hypoglycemia with intravenous 20% glucose infusion, metabolic acidosis progressed. Continuous hemodiafiltration was performed for 12 h to improve severe acidosis. Urinary organic acid analysis showed increased excretion of dicarboxylic acid. In total, 5 μl serum was used for acylcarnitine analysis using NeoSMAAT kit (cat. nos. 509254, 509261 and 509278; https://www.sekisui-medical.jp/business/diagnostics/others/neosmaat/; Sekisui Medical Co., Ltd.) and the LCMS-8040 instrument (Shimadzu Corporation). Her metabolic state was stabilized within 2 days from the onset and she recovered with no neurological complications.

On the day of symptom onset, in November 2014, patient 2 was 6 months old. He had a low-grade fever and showed loss of appetite. The next day, he began having diarrhea and vomited three times in the evening. After showing impaired consciousness 2 days later, the first blood test was performed. Ultrasonography revealed an enlarged and fatty liver. He was transferred to Fujita Health University Hospital (Toyoake, Japan), where continuous hemodiafiltration was performed for 18 h in a similar procedure to that performed on patient 1. In total, 6 μl serum was used for acylcarnitine analysis using MS^2 Screening Neo II kit (https://www.siemens-healthineers.com/jp/newborn-mass-screening/ms2-screening-series; Siemens Healthineers) and API 3200™ LC-MS/MS System (SCIEX). He recovered without neurological complications, similar to patient 1.

On the day of symptom onset, in October 2015, patient 3 was 7 months old. He appeared drowsy in the afternoon and then gradually developed tachypnea and loss of appetite. The next morning, the first blood examination was performed and hepatomegaly was identified at Kitasato University Hospital (looked after by KA; Sagamihara, Japan). Two dried blood spots were used for acylcarnitine analysis using MS^2 Screening Neo II kit (https://www.siemens-healthineers.com/jp/newborn-mass-screening/ms2-screening-series; Siemens Healthineers) and API 3200™ LC-MS/MS System (SCIEX). A computed tomography scan revealed an enlarged and fatty liver. Hypoglycemia was immediately corrected by glucose infusion. Metabolic acidosis was corrected by continuous bicarbonate infusion (about 2 mEq/kg/h) for 5 h. He recovered without neurological complications.

As a newborn, patient 4 was fed with both breast milk and infant formula and showed normal physical growth until 3 months of age. Thereafter, she was fed with only breast milk and her physical growth and development slowed down. On the day of symptom onset, in November 2016, she was 7 months old. She vomited twice around noon and then gradually developed tachypnea and impaired consciousness. She was hospitalized at Kurume University Hospital (Kurume, Japan) early the next morning because of severe hypoglycemia and metabolic acidosis. An infusion of glucose and bicarbonate was started immediately. The patient's enlarged liver showed homogeneous hyperechogenicity compared with the kidney, which suggested a fatty liver. After 11 h, her metabolic status and consciousness had almost fully recovered. In total, 6 μl serum was used for acylcarnitine analysis using Quattro Premier MS/MS (cat. no. 7200000594; Waters Coporation). Labeled carnitine standards set B-op (cat. no. NSK-B-OP-1; Otsuka Pharmaceutical Co., Ltd.) was used as internal standards.

In all 4 cases, urinary organic acids were analyzed using GCMS-QP2010 Plus (Shimadzu Corporation). Urine samples containing 0.1 mg creatinine were used for this analysis. In Patient 4, QP5050 GC/MS (Shimadzu Corporation) was also used for confirmation. Urine sample containing 0.2 mg creatinine was used for this analysis. Urine samples were prepared according to the previous report (14). The mass/charge ratios (*m/z*) used to detect 4-HMP were 73, 99, 127, 139, 155, 170, 183 and 198 (10). The details of blood acylcarnitine analyses were summarized in Table SI.

On first evaluation, the results of urinary organic acid analyses and blood acylcarnitine profiles in the acute phases of all four cases were regarded as non-specific. Patients 1, 2 and 3 were suspected of having *HMGCS2* deficiency, because they presented with hypoketotic hypoglycemia and a high ratio of FFAs/TKBs, which prompted sequencing of their *HMGCS2* alleles immediately. In the case of patient 4, because the value of TKBs during hypoglycemia was unknown, a gene panel analysis was instead performed. After their critical episode,

Table I. Laboratory findings from a single blood sample taken during hypoglycemic crisis in each of the four patients with *HMGCS2* variants.

			Laboratory findings									Mutation in *HMGCS2*	
Patient	Sex	Age of onset months	pH	BE mM	Glucose mM	TKBs mM	FFAs mM	FFAs/TKBs	Glucose x TKBs	AST IU/l	ALT IU/l	C0 μM	C2 μM	C2/C0	Allele 1	Allele 2
1	F	8	7.02	-26.8	0.78	0.502	3.32	6.6	0.39	358	173	20.6	56.1	2.72	p.S392L	p.R500H
2	M	6	6.95	-28.9	1.17	0.4	2.5	6.3	0.47	241	140	8.03	75.8	9.44	p.G219E	p.R500C
3	M	7	7.13	-24.4	1.83	0.161	2.20	13.7	0.29	230	156	8.75	53.4	6.10	p.M235T	p.S392L
4	F	7	6.92	-29.7	1.11		2.39			193	154	10.9	23.0	2.12	p.M235T	p.V253A

M, male; F, female; BE, base excess; TKBs, total ketone bodies; FFAs, free fatty acids; AST, aspartate aminotransferase; ALT, alanine aminotransferase; C0, free carnitine; C2, acetylcarnitine. For acylcarnitine analysis, serum was used from patients 1, 2 and 4 and a dried blood spot was used from patient 3.

each patient was advised to avoid prolonged fasting and to receive glucose infusion prophylactically during anorexia, to prevent another hypoglycemic episode. Patients 1, 2 and 4 have been followed for 6, 5 and 3 years, respectively. They have grown and developed normally without neurological sequelae and fatty liver disappeared in all three. No data were obtained regarding the prognosis of patient 3 due to the loss of follow-up.

Mutational analysis. To obtain the white blood cells, ~4 ml whole blood sample was added to an equivalent volume of solution consisting of 3% (W/V) dextran and 0.9% (W/V) NaCl, which was incubated for 1 h at room temperature to precipitate the red blood cells and to obtain the supernatant. The supernatant was then centrifuged at 1,730 x g for 10 min at room temperature to precipitate the white blood cells. Genomic DNA was purified from the white blood cells using a Sepa Gene kit (EIDIA Co., Ltd.) following the manufacturer's protocol. The genomic *HMGCS2* sequence was obtained from the National Center for Biotechnology (NCBI) Reference Sequence Database (accession no. NG_013348.1/NM_005518.3). The 10 exons of *HMGCS2* from patients 1, 2 and 3 were amplified by PCR using a TaKaRa Taq™ (Takara Bio Inc.) and flanking intronic primers (listed in Table SII) under the following thermocycling conditions: Initial denaturation at 94˚C for 1 min, followed by 35 cycles of 94˚C for 1 min, 54˚C for 1 min and 72˚C for 1 min. DNA electrophoresis in 2% agarose gel was used to verify successful amplification. The amplified DNA in the gel was visualized with EtBr solution (cat. no. 315-90051; Nippon Gene Co., Ltd.). Each amplified DNA was sequenced by bidirectional Sanger sequencing using BigDye™ Terminator v1.1 Cycle Sequencing kit (cat. no. 4337450; Applied Biosystems; Thermo Fisher Scientific, Inc.) and a 3130*xl* Genetic Analyzer (Applied Biosystems; Thermo Fisher Scientific, Inc.). The same primers as those listed in Table SII were used to sequence the amplified DNA.

In the case of Patient 4, the NextSeq Sequencing System (Illumina, Inc.) at the Kazusa DNA Research Institute (Kisarazu, Japan) was used to perform a mutation analysis based on a DNA panel consisting of 193 genes (Table SIII). In the present study, additional 25 genes were added to a previous DNA panel containing 168 genes to detect various inherited metabolic diseases, including fatty acid oxidation, ketone body metabolism and transport and glycogen storage diseases (15). The customized probe was designed for target enrichment of the panel genes by SureSelect DNA Advanced Design Wizard (v5.5; https://earray.chem.agilent.com/suredesign/) and obtained from Agilent technologies, Inc. (cat. no. 5190-4859; Agilent technologies, Inc.). Because genomic DNA was subjected to enzymatic fragmentation using a KAPA hyperplus library construction kit (cat. no. KK8510; Roche Diagnostics) for Illumina short-read next-generation sequencing, the insert DNA size of the resultant library, but not the integrity of genomic DNA, was monitored on a MultiNA microchip electrophoresis system (cat. no. MCE®-202; Shimadzu Corporation). DNA sequencing was done using a NextSeq 500/550 Mid Output kit v2.5 (75 bp paired end; 150 cycles; cat. no. 20024904; Illumina, Inc.) using a NextSeq 500 system (Illumina, Inc.). The loading concentration of the library was 1.8 pM, which was quantified with a KAPA library quantification kit (cat. no. KK4824; KAPA Biosystems;

Roche Diagnostics). Variants in protein-coding exonic regions and their 10-base flanking regions were detected with the pipeline that was previously described (15). Briefly, sequence reads were aligned with the reference human genome (hg38; GCA_000001405.2) using the Burrows-Wheeler Aligner 'MEM' v0.7.5a35 algorithm (16). The duplicate reads were removed using Picard-1.84's 'MarkDuplicates' command (http://broadinstitute.github.io/picard/). SNPs and indels were called using VarScan2's v.2.3.3 (http://varscan.sourceforge.net) (17) and Genome Analysis Toolkit-3.6.0 (GATK) HaplotypeCaller and UnifiedGenotyper (18,19).

In silico analysis of identified novel rare variants in the *HMGCS2* gene was performed for all 4 cases using MutationTaster (https://www.mutationtaster.org/) (20), Polymorphism Phenotyping version 2 (http://genetics.bwh.harvard.edu/pph2/), Protein Variation Effect Analyzer (PROVEAN) and Sorting Intolerant from Tolerant (SIFT) (11 Dec, 2019; https://provean.jcvi.org/index.php).

Construction of two HMGCS2 expression vectors: One eukaryotic and one prokaryotic. The first step was to clone wild-type full-length *HMGCS2* cDNA (NCBI sequence no.: NM_005518.3), which contains a mitochondrial targeting sequence, into the *Eco*RI site of the eukaryotic expression vector pCAGGS (21), which was performed by DNA Synthesis Services (GenScript Japan, Inc.). Next, the cDNA fragment encoding *HMGCS2* without the mitochondrial targeting sequence was amplified by PCR from the eukaryotic expression vector using KOD FX Neo (Toyobo Life Science) and primers containing *Bam*HI and *Eco*RI restriction sequences (italics), respectively: Forward, 5'-CGC*GGATCC*CTGGAAGTTCTG TTCCAGGGTCCTACAGCCTCTGCTGTCC-3'; and reverse, 5'-GAGGAGT*GAATTC*TTAAACGG-3' under the following cycling conditions: Initial denaturation at 95˚C for 2 min, followed by 45 cycles of 98˚C for 10 sec, 58˚C for 30 sec and 68˚C for 45 sec. The underlined segment of the forward primer is the recognition sequence of PreScission protease (GE Healthcare), which was used in subsequent experiments. The amplified fragment was digested by *Bam*HI and *Eco*RI, then subcloned into the bacterial expression vector pGEX-6P-1 (GE Healthcare), which included the coding sequence of the fusion protein glutathione s-transferase (GST). The synthesized constructs were transformed into the *E. coli* strain JM109 (Toyobo Life Science). Positive clones were confirmed by the Sanger method and agarose gel electrophoresis to analyze the size of DNA fragments after enzymatic digestion of plasmid DNA (data not shown). These plasmid constructs were purified by an Automatic DNA Isolation system PI-50 (Kurabo Industries, Ltd.) and stored for subsequent experiments. The simplified map of the bacterial expression vector is illustrated in Fig. S1. A pGEX-6P-1 empty vector was used for the expression of an isolated GST protein. Each variant was introduced into the two *HMGCS2* expression vectors (one eukaryotic and one prokaryotic) using a KOD-Plus mutagenesis kit and KOD-Plus-Neo by following the manufacturer's instructions (Toyobo Life Sciences, Ltd.).

Transient expression of HMGCS2 in HEK293T cells and western blotting. 293T cells (RIKEN Bioresource Center) were used for expression experiments. Mycoplasma testing was done using an EZ-PCR Mycoplasma test kit (Biological Industries) according to the manufacturer's instructions. Each eukaryotic expression construct (2 μg) containing wild-type or variant *HMGCS2*, or empty vector was transfected into $3x10^5$ 293T cells using Lipofectamine® 2000 (Thermo Fisher Scientific, Inc.). After 1 day, the transfected cells were lysed with 200 μl hypotonic lysis buffer (10 mM Tris-HCl, 10 mM NaCl, 0.5% Triton X-100, 10 mM EDTA, pH 7.5). Protein in the soluble fraction was quantified by the Bradford protein assay using Bio-Rad Protein Assay Dye Reagent Concentrate (cat. no. 500-0006; Bio-Rad Laboratories, Inc.) (22). Each protein sample (HMGC2, 20 μg; β-actin, 5 μg) was subjected to electrophoresis in a 10% polyacrylamide gel containing sodium dodecyl sulfate (SDS-PAGE), then transferred to 0.2-μm PVDF membrane using iBlot 2 Dry Blotting System (Thermo Fisher Scientific, Inc.). The membranes were then blocked in TBS supplemented with 0.1% Tween 20 and 5% BSA (cat. no. 015-21274; FUJIFILM Wako Pure Chemical Corporation) for 70 min at room temperature. The membranes were probed with a rabbit polyclonal antibody (1:795; cat. no. ab104807; Abcam) against a synthetic peptide corresponding to a region within C-terminal amino acids 444-493 of human HMGCS2 (NCBI reference sequence: NP_005509) or a monoclonal anti-β-actin antibody produced in mouse (1:10,000; cat. no. A5441; Sigma-Aldrich; Merck KGaA) for 1 h at room temperature. This is followed by incubation with the secondary antibodies for 1 h at room temperature and Amersham™ ECL™ Prime Western Blotting Detection Reagent (GE Healthcare) for detection. The secondary antibody used to detect HMGCS2 was horseradish peroxidase (HRP)-conjugated anti-rabbit IgG H + L (cat. no. W4011; Promega Corporation), whilst that used to detect β-actin was Amersham ECL sheep anti-mouse IgG, HRP-linked whole Ab (cat. no. NA931-1ML; Cytiva). Both antibodies had been diluted to 1:10,000 before use.

Expression in E. coli, purification and western blotting of HMGCS2. Wild-type and mutant HMGCS2 expression vectors were transformed into the *E. coli* strain BL21 (DE3; BioDynamics Laboratory Inc.) grown in lysogeny broth (LB) medium (0.5% NaCl, 1% tryptone and 0.5% yeast extract; Thermo Fisher Scientific, Inc.) containing 0.1 mg/ml ampicillin to an A600 of 0.9-1.1 at 37˚C. Optimal protein expression was induced with 0.3 mM isopropyl-β-D-thiogalactopyrano side (FUJIFILM Wako Pure Chemical Corporation) at 18˚C for 16 h. Cells were recovered by centrifugation at 1,800 x g at 4˚C for 10 min, resuspended in lysis buffer A [50 mM HEPES, 200 mM NaCl, pH 7.5, 10% glycerol, 1 mM dithiothreitol (DTT), 1.1 mM 4-(2-Aminoethyl)-benzenesulfonyl fluoride] and disrupted by sonication at 0˚C, with 10-sec sonications repeated 25 times. The interval between each sonication was 50 sec. After centrifugation at 15,000 x g at 4˚C for 30 min, the soluble fraction was loaded into a column containing Glutathione Sepharose 4 Fast Flow (GE Healthcare) before the column was washed with lysis buffer B (50 mM HEPES, 200 mM NaCl, pH 7.5, 10% glycerol, 1 mM DTT) followed by wash buffer (50 mM HEPES, 200 mM NaCl, pH 7.5, 10% glycerol, 1 mM DTT, 0.5% [v/v] Triton X-100). Triton X-100 was removed by washing the column again with lysis buffer B. The GST fusion protein was eluted from the column

using elution buffer (50 mM Tris-HCl, 9.8 mM reduced glutathione, pH 8.0). After exchanging the buffer with cleavage buffer (50 mM Tris-HCl, 150 mM NaCl, 1 mM EDTA, pH 7.5, 1 mM DTT) by filtration and dialysis, GST was separated from HMGCS2 by treatment with PreScission protease (GE Healthcare) at 4˚C for 12 h. PreScission protease and separated GST were removed from the mixture by running it through the Glutathione Sepharose 4 Fast Flow column again. Purified HMGCS2 was quantified by absorbance at 280 nm using a NanoDrop™ 1,000 Spectrophotometer (Thermo Fisher Scientific, Inc.). An isolated GST protein was created using the same procedure for HMGCS2 proteins. To compare the purity of each enzyme, 600 ng each partially purified wild-type or variant HMGCS2 was separated by 10% SDS-PAGE transferred onto a nitrocellulose membrane. The membrane was used for Ponceau staining and subsequent Western blotting. TBS supplemented with 5% BSA was used as the blocking agent. The nitrocellulose membrane was then blocked for 3 h at room temperature. The membrane was probed with a rabbit polyclonal antibody (cat. no. ab104807; Abcam) against a synthetic peptide corresponding to a region within C-terminal amino acids 444-493 of human HMGCS2 (NCBI reference sequence: NP_005509) for 17 h at room temperature before being probed with the alkaline phosphatase-conjugated anti-rabbit IgG (Fc) secondary antibody, (1:7,500; cat. no. S3731; Promega Corporation) for 70 min at room temperature.

In another experiment, 450 ng each sample was separated by 10% SDS-PAGE before the proteins in the gel were stained with Coomassie brilliant blue R-250 (cat. no. 031-17922; FUJIFILM Wako Pure Chemical Corporation) for 20 min at room temperature. These samples were not transferred onto a membrane.

Enzymatic activity assay for purified HMGCS2. The spectrophotometric method described by Clinkenbeard *et al* (23) was used with modifications. Each protein sample (16.4-43.2 μg) was incubated in 900 μl enzyme assay buffer (100 mM Tris-HCl, 100 μM EDTA, 0.2% v/v Triton X-100, pH 8.2) containing 300 μM acetyl-CoA (Sigma-Aldrich; Merck KGaA) for 17 min at 30˚C to prevent inactivation of HMGCS2 by succinylation (24,25). Next, 35 nmol acetoacetyl-CoA (Sigma-Aldrich; Merck KGaA) were added, where HMGCS2 activity was calculated from the rate of decrease of acetoacetyl-CoA measured by spectrophotometry at 300 nm, at which the absorbance of the enolate form of acetoacetyl-CoA was maximum (26). The molar extinction coefficient of acetoacetyl-CoA is $3.6x10^3$ in this enzyme assay buffer (23). Activity measurements were performed in three independent experiments. Data are expressed as the mean ± SD.

Statistical analysis. One-way analysis of variance (ANOVA) with Dunnett's multiple comparison test was performed using Prism 8 software (GraphPad Software, Inc.) to compare enzyme activities. $P<0.05$ was considered to indicate a statistically significant difference.

Results

Mutational analysis. Six rare, non-synonymous variants of *HMGCS2* were detected in the four study cases, comprising compound heterozygotes of two variants (Fig. S2; Table I). Two of the variants, c.704T>C (p.M235T) and c.1175C>T (p.S392L), were identified in two unrelated patients. Five of the variants are novel mutations: c.656G>A (p.G219E), c.704T>C (p.M235T), c.758T>C (p.V253A), c.1175C>T (p.S392L), and c.1498C>T (p.R500C). Only the c.1499G>A (p.R500H) variant had been reported previously as a pathogenic mutation (27,28). In the mutation analysis of patient 4, the presence of any rare variants in other genes known to be related to abnormal blood glucose levels was not observed (Table SIII). All five of the novel *HMGCS2* variants were evaluated *in silico* by MutationTaster, PolyPhen-2, PROVEAN and SIFT to be disease-causing, probably damaging, deleterious and damaging, respectively.

Transient expression and immunoblotting of HMGCS2 in 293T cells. Full-length *HMGCS2* cDNA contains a mitochondrial targeting sequence. HMGCS2 is expressed in cytosol as an immature protein with mitochondrial targeting peptide, which is cleaved in the mitochondrial matrix (5,29). Western blot analysis confirmed that immature HMGCS2 protein with mitochondrial targeting peptide was expressed in all transfected cells except for the empty vector-transfected cells, and each expression level was similar (upper-band of the suitable molecular weight of immature HMGCS2 protein with mitochondrial targeting peptide). This result indicated by the western blot analysis suggested that each transfection was successful (Fig. 1). An antibody against β-actin was used as a protein loading control, confirming that the amount of proteins in applied samples were similar (Fig. 1). The levels of mutant M235T, R500C and R500H proteins without mitochondrial targeting peptide were clearly detectable (lower-band). However, mutant G219E protein without mitochondrial targeting peptide was not detectable, even though immature protein with mitochondrial targeting peptide was detected, as were wild-type and other mutants.

Expression and purification of HMGCS2 from E. coli. A wild-type HMGCS2-GST fusion protein that was expressed in *E. coli* was successfully constructed. Wild-type HMGCS2 protein was then purified using Glutathione Sepharose column chromatography, PreScission protease cleavage and a second Glutathione Sepharose column (Fig. S3). Although extra protein bands remained in the purified wild-type HMGCS2 preparation, a further purification step decreased its enzyme activity, this partially purified preparation was used in the enzymatic activity assay. From 1 g of cultured *E. coli* 147 μg of wild-type HMGCS2 was purified.

The variant HMGCS2 proteins were expressed and purified using the same procedure. The amounts of purified proteins (μg) obtained from 1 g of *E. coli* expressing the HMGCS2 variants G219E, M235T, V253A, S392L and R500C were 42.2, 258, 147.8, 66.5 and 99.6, respectively.

Fig. 2A-C shows western blotting results, ponceau staining and coomassie brilliant blue R-250 staining of each partially purified HMGCS2. The G219E variant had a weaker signal compared with the wild-type and other HMGCS2 variants, indicating that the purity of the G219E preparation was lower than the others (Fig. 2A). The enzymatic activity of the wild-type, V253A, R500C and S392L HMGCS2 were

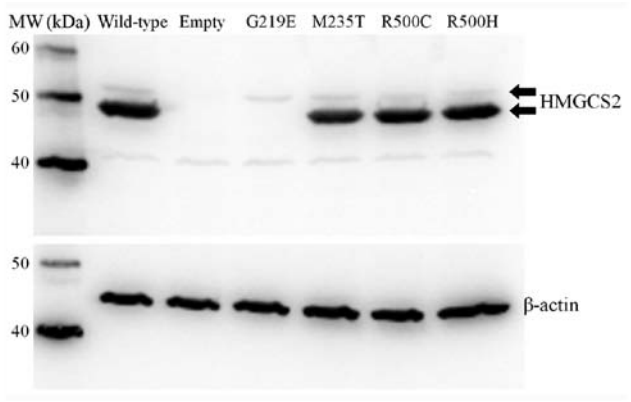

Figure 1. Immunoblot analysis of transiently expressed wild-type and variant HMGCS2 in 293T cells. Protein samples from 293T cells transfected with wild-type or mutant *HMGCS2* cDNA or empty expression vectors were probed with anti-human HMGCS2 antibody and monoclonal anti-β-actin antibody. The upper arrow indicates HMGCS2 with mitochondrial targeting peptide, and the lower arrow indicates HMGCS2 without mitochondrial targeting peptide. HMGCS2, 3-hydroxy-3-methylglutaryl-CoA.

345±58.2, 83±8.45, 12.7±1.30, and 3.6±3.43 nmol/min/mg protein, respectively, and these activities of the variants were significantly lower than that of wild-type. Only the V253A variant had some residual activity. The other four variants had either no detectable activity or negligible enzymatic activity. (Fig. 2D). Based on these expression analyses, it was concluded that all five variants were pathogenic.

Discussion

In the present report, four cases of *HMGCS2* deficiency have been described in Japanese patients. All four patients presented with severe hypoketotic hypoglycemia with severe metabolic acidosis, hepatomegaly or fatty liver with elevated liver enzymes, elevated C2 and C2/C0 ratio in acylcarnitine analysis and an elevated FFA level during an acute episode of metabolic decompensation (Table I). Although the TKBs measurement during the acute episode in Patient 4 was not available, the other three patients had high FFAs/TKBs ratios. Genetic analyses revealed that these patients were compound heterozygotes of two variants. Five out of the six identified variants were novel variants (Table I). Initially a transient expression analysis of wild-type and variant HMGCS2 was conducted in human fibroblasts, which was established and SV40-transformed in the laboratory from a patient with beta-ketothiolase deficiency and used in previous report (30). In this earlier study it was difficult to detect wild-type HMGCS enzyme activity. Using a bacterial expression system that was previously used for characterization of HMGCS2 mutants by other groups (28,31) it was possible to confirm that these novel variants are disease-causing missense mutations. The p.G219E mutant enzyme appeared to be less stable than the wild-type enzyme, which was also confirmed by the transient expression experiment in HEK293T cells.

Clinically it is still challenging to recognize *HMGCS2* deficiency (10). A non-ketotic hypoglycemic episode with a high FFAs/TKBs ratio is the most important feature of *HMGCS2* deficiency as well as defects in fatty acid oxidation (6). Each fatty acid oxidation defect has a characteristic profile in blood

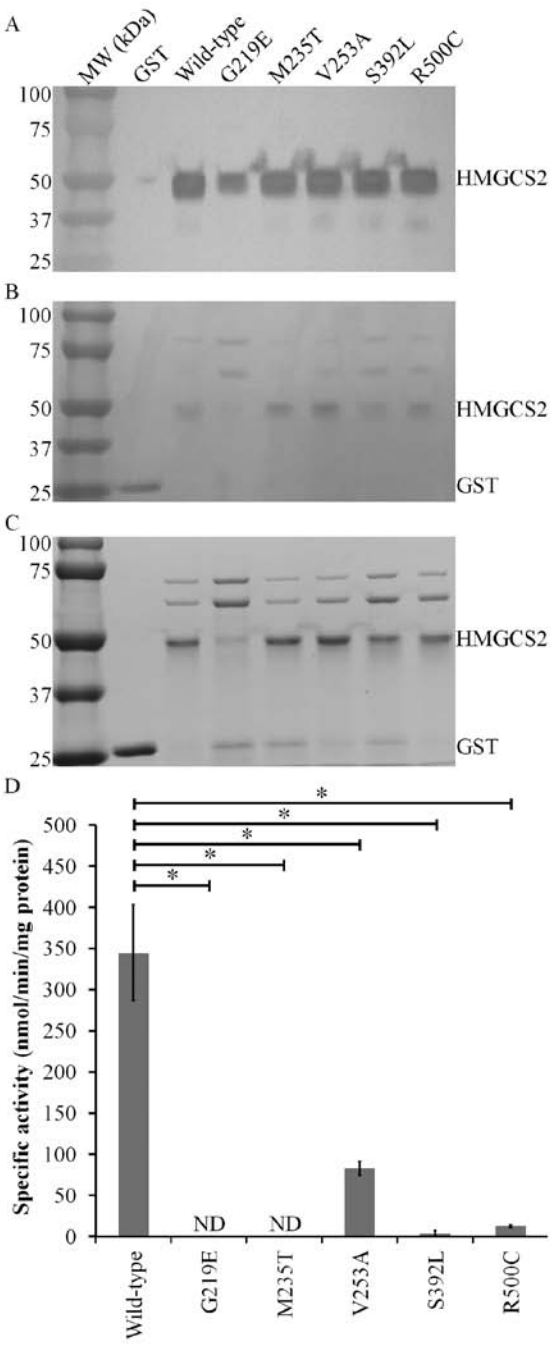

Figure 2. HMGCS2 expression in a bacterial system. The purified GST protein was used as a negative control. (A) Western blotting of 600 ng purified wild-type and variant HMGCS2 expressed and purified from *Escherichia coli* and probed with anti-human HMGCS2 antibody. (B) Ponceau staining was performed on the same membrane used for the immunoblot and shows equal protein loading and transfer. (C) Coomassie brilliant blue R-250 staining of 450 ng of each sample shows equal distribution of proteins in the gel. (D) Specific enzymatic activity (dark gray bars) of wild-type and the G219E, M235T, V253A, S392L and R500C mutant variants of HMGCS2. Activity measurements were performed in three independent experiments. The error bars indicate standard deviations. Significant differences were observed compared to wild-type. *P<0.0001. HMGCS2, 3-hydroxy-3-methylglutaryl-CoA; ND, not detected.

acylcarnitine analysis (32). In cases of *HMGCS2* deficiency, some reports have described that elevated C2 and C2/C0 ratios were observed during acute episodes (11,12,33). In the present study high C2 and relatively low C0 was also observed in the

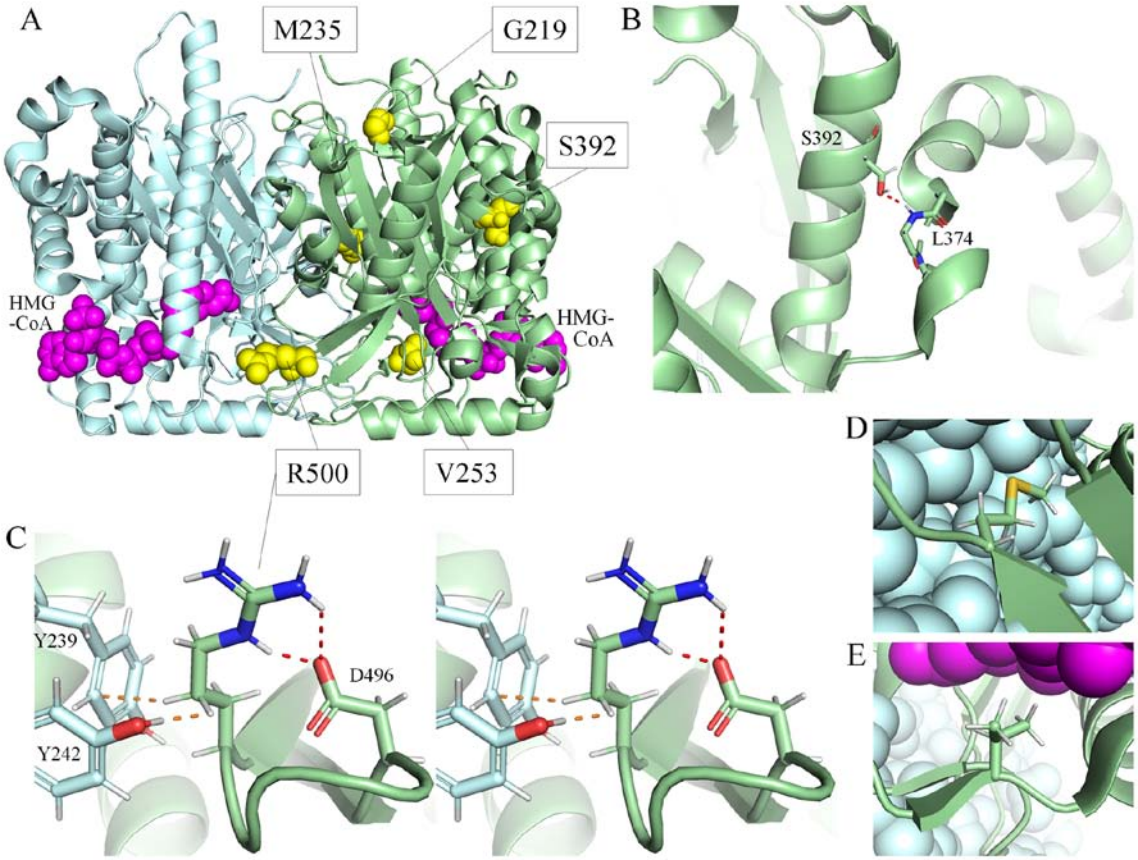

Figure 3. Three-dimensional structure of HMGCS2, obtained using PyMOL Molecular Graphics System version 2.2.0. (A) The whole structure of wild-type HMGCS2, shown as a homodimer. Each subunit is indicated by a green or cyan ribbon diagram. The residues substituted in patients are shown as yellow spheres. HMG-CoA is indicated by magenta spheres. (B) A partial structure of wild-type HMGCS2. Ser392 and the main chain of Leu374 are shown as a stick model colored by atom type (cyan or green, C; red, O; blue, N; white, H; and gold, S). The hydrogen bond between Ser392 and Leu374 is shown as a dotted red line. (C) A partial structure of wild-type HMGCS2 in cross-eye stereo view. The side chains of Asp496 and Arg500, and those of Tyr239 and Tyr242 in another subunit, are shown as a stick model. Hydrogen bonds are shown as dotted red lines. The side chain of Arg500 forms two hydrogen bonds with Asp496. Arg500 is also exposed to Tyr239 and Tyr242 in another subunit. The shortest interatomic distances to Arg500 from Tyr242 and Tyr239 (shown as dotted orange lines) are 170 and 280 picometers, respectively. (D) The side chain of Met235 shown as a stick model. Cyan spheres indicate another subunit. (E) The side chain of Val253 shown as a stick model. HMG-CoA is indicated by magenta spheres. Cyan spheres indicate another subunit. HMGCS2, 3-hydroxy-3-methylglutaryl-CoA.

patients. In *HMGCS2* deficiency, the β-oxidation pathway is intact and produces plenty of acetyl-CoA in times of ketogenic stress, but acetyl-CoA cannot be used for ketogenesis. Hence, it is reasonable that acetyl-CoA is accumulated and produces acetylcarnitine (C2) in hepatocytes. However, in patients with fatty acid oxidation defects, acetyl-CoA production via β-oxidation is impaired. It may be hypothesized that hypoketotic hypoglycemia with elevated C2 and C2/C0 ratios during an acute crisis may be a promising indicator to identify *HMGCS2* deficiency. Urinary organic acid analysis shows non-ketotic dicarboxylic aciduria in both *HMGCS2* deficiency and fatty acid oxidation defects. Recently, Pitt *et al* (10) reported the presence of characteristic urinary organic acids such as 4HMP during acute episodes in patients with *HMGCS2* deficiency. Retrospectively, 4HMP was also detected in the urine samples of the patients in the present study. It should be stressed that such findings are only detected during acute episodes in both acylcarnitine and urinary organic acid analyses (10).

Enzymatic assay of HMGCS2 activity is reported to be challenging (5) and is currently measured by the reduction of acetoacetyl-CoA spectrophotometrically (13,28,31,34). However, another cytosolic form of HMGCS and several other enzymes may influence the assay because these enzymes utilize acetoacetyl-CoA (34). The latter might include mitochondrial acetoacetyl-CoA thiolase, mitochondrial 3-ketoacyl-CoA thiolase, cytosolic acetoacetyl-CoA thiolase, and acyl-CoA hydrolase. Lascelles and Quant (34) measured HMGCS2 activity in human liver samples. Whole lysates of transfected SV40-transformed fibroblasts, which were derived from a patient with mitochondrial acetoacetyl-CoA thiolase (T2) deficiency (30) and chosen because T2 is one of the major enzymes that catalyzes acetoacetyl-CoA and thus could affect the HMGCS2 enzyme assay, failed to show HMGCS2 enzymatic activity. The expression level of HMGCS2 protein might have been too low to overcome the other intrinsic enzymes that use acetoacetyl-CoA as a substrate.

When the research strategy was changed to assay the activity of HMGCS2 purified from a bacterial expression system influences from other enzymes no longer needed to be considered. Previously two reports described the successful characterization of HMGCS mutants using bacterial expression systems (28,31). In the bacterial expression

system in the present study, enzyme assays were performed without adding Mg^{2+}. Mg^{2+} can increase the absorbance of acetoacetyl-CoA (26), but it inhibits HMGCS2 in a concentration-dependent manner; for example, 10 mM Mg^{2+} in the assay buffer inhibits the reaction by 50% (35). The concentration of free Mg^{2+} in the matrix of liver mitochondria is estimated to range from 0.8 to 1.2 mM (36), so the *in vivo* inhibition effect of Mg^{2+} would seem to be quite small. While adopting this physiological concentration of Mg^{2+} would have been ideal, a reliable molar extinction coefficient of acetoacetyl-CoA at this physiological condition was not found in the literature. Thus, in the present study no Mg^{2+} was added to the enzyme assay buffer, even though a previous report adopted 5-10 mM Mg^{2+} (34).

Enzymatic activity of the V253A variant was approximately one quarter that of the wild-type enzyme, which was much higher than the other four variants. The V253A variant was found in patient 4. Patient 4 C2/C0 and C2 (acetylcarnitine) levels were the lowest of all four patients, which is compatible with the fact that this variant showed some residual activity in the experiments. It may be hypothesized that a small amount of acetyl-CoA in hepatocytes was transformed into ketone bodies in Patient 4 by the V253A variant. The data suggest that the V253A variant may be a disease-causing mutation. It shows lower enzymatic activity than the R505Q variant, which was reported to be a disease-causing mutation (31).

The enzyme kinetics of HMGCS2 were also challenging. The V253A variant showed some residual activity, which led to further analysis. Kinetic analysis of the V253A variant and wild-type protein was performed. However, K_m values for acetoacetyl-CoA were too low to be evaluated accurately (data not shown). An attempt to identify the K_m value for acetyl-CoA was also made. The K_m value for acetyl-CoA in this experiment was higher compared with that described previously (data not shown) (28). This could be because large amounts of acetyl-CoA were consumed during preincubation. Enzyme kinetics of the variant should be further researched to elucidate its pathophysiology in more detail.

The three-dimensional structure of human HMGCS2 (Protein Databank ID: 2WYA) is shown in Fig. 3A. In this structure, two subunits form a homodimer, which is crucial for its enzymatic activity (31). The residues Glu132, Cys166 and His301 catalyze the reaction directly (37). The residues Ser392 and Leu374, each a part of an α-helix, are connected by the only hydrogen bond between these two alpha-helices (Fig. 3B). Replacing Ser392 with a Leu residue (S392L) would remove this hydrogen bond and may alter the tertiary structure of HMGCS2. Arg500 is located on the neighbor region of a beta-turn, and is also located on the dimerization surface. Because the side chain of Arg500 forms two hydrogen bonds with Asp496 (Fig. 3C), this beta-turn may become unstable when these hydrogen bonds are lost due to the replacement of Arg500 with Cys (variant R500C), which also could affect dimerization. Met235 is located on the dimerization surface (Fig. 3D). Because replacement of this amino acid with Thr (M235T) would change the hydrophilicity of this surface, it may affect dimerization. Val253 is one of the residues that compose the active site of this enzyme (Fig. 3E), but is not directly involved in the chemical reaction. Replacing this amino acid with Ala (V253A) could alter the interaction of residues that compose the active site, and would make it difficult to stabilize the substrates in an appropriate position. In summary, the secondary structure may be affected by R500C, the tertiary structure may be affected by S392L, the quaternary structure may be affected by M235T and R500C and the V253A variant would be expected to affect the binding to substrates.

In conclusion, *in vitro* analysis has shown that the p.G219E, p.M235T, p.V253A, p.S392L and p.R500C variants of *HMGCS2* are disease-causing mutations. In acylcarnitine analysis, C2 and C2/C0 in the acute phase may be promising indicators to differentiate *HMGCS2* deficiency from fatty acid oxidation defects.

Acknowledgements

The authors would like to express gratitude to Ms Naomi Sakaguchi and Ms Sachie Hori, the Department of Pediatrics, Gifu University (Gifu, Japan) assisted in these experiments as laboratory assistants. Dr. Yuki Hasegawa of the Department of Pediatrics, Shimane University Faculty of Medicine (Izumo, Japan) confirmed the mas spectra of 4-HMP in all urine samples.

Funding

This research was supported in part by a Grant-in-Aid for Scientific Research from the Ministry of Education, Culture, Sports, Science and Technology of Japan (grant no. 16K09962) and by grants from Japan Agency for Medical Research and Development (grant no. JP17ek0109276), Health and Labor Sciences Research Grants [H29-nanchitou(nan)-ippan-051] for Research on Rare and Intractable diseases and The Morinaga Foundation for Health & Nutrition.

Availability of data and materials

The datasets generated and/or analyzed during the current study are available in the Figshare repository (https://doi.org/10.6084/m9.figshare.10308536.v1). All datasets are additionally available from the corresponding author on reasonable request.

Authors' contributions

KA, KF, YW, YN and TI were involved in clinical management of the patients. MN, YA, HS, HM, RF and OO were involved in mutation analysis. YA, HO, EA and HO were involved in expression analyses. YA wrote the first draft of the manuscript. TF initiated and supervised the study and reviewed and revised the manuscript. All authors approved the final manuscript for submission to this journal and agree to be accountable for all aspects of the work.

Ethics approval and consent to participate

This study was approved by the Ethical Committee of the Graduate School of Medicine, Gifu University, Japan and was carried out in accordance with the principles contained within the Declaration of Helsinki. Informed consent was obtained from the parents of all patients.

Patient consent for publication

All parents of the patients agreed to the publication of these data without identifying information by signing informed consent.

Competing interests

The authors declare that they have no competing interests.

References

1. Mitchell GA and Fukao T: Inborn errors of ketone body metabolism. In: The metabolic & molecular basis of inherited disease. Scriver CR, Beaudet AL, Sly WS and Valle D (eds.). McGraw-Hill, New York, pp2327-2356, 2001.
2. Sass JO: Inborn errors of ketogenesis and ketone body utilization. J Interit Metab Dis 35: 23-28, 2012.
3. Hegardt FG: Mitochondrial 3-hydroxy-3-methylglutaryl-CoA synthase: A control enzyme in ketogenesis. Biochem J 338: 569-582, 1999.
4. Williamson DH, Bates MW and Krebs HA: Activity and intracellular distribution of enzymes of ketone-body metabolism in rat liver. Biochem J 108: 353-361, 1968.
5. Boukaftane Y and Mitchell GA: Cloning and characterization of the human mitochondrial 3-hydroxy-3-methylglutaryl CoA synthase gene. Gene 195: 121-126, 1997.
6. Fukao T, Mitchell G, Sass JO, Hori T, Orii K and Aoyama Y: Ketone body metabolism and its defects. J Inherit Metab Dis 37: 541-551, 2014.
7. Wolf NI, Rahman S, Clayton PT and Zschocke J: Mitochondrial HMG-CoA synthase deficiency: Identification of two further patients carrying two novel mutations. Eur J Pediatr 162: 279-280, 2003.
8. Carpenter KH, Bhattacharya K, Ellaway C, Zschocke J and Pitt JJ: Improved sensitivity for HMG CoA synthase detection using key markers on organic acid screen. J Inherit Metab Dis 33: S62, 2010.
9. Sass JO, Kuhlwein E, Klauwer D, Rohrbach M and Baumgartner MR: Hemodiafiltration in mitochondrial 3-hydroxy-3-methylglutaryl coenzyme A synthase (HMG-CoA synthase) deficiency. J Inherit Metab Dis 36 (Suppl 2): S189, 2013.
10. Pitt JJ, Peters H, Boneh A, Yaplito-Lee J, Wieser S, Hinderhofer K, Johnson D and Zschocke J: Mitochondrial 3-hydroxy-3-methylglutaryl-CoA synthase deficiency: Urinary organic acid profiles and expanded spectrum of mutations. J Inherit Metab Dis 38: 459-466, 2015.
11. Conboy E, Vairo F, Schultz M, Agre K, Ridsdale R, Deyle D, Oglesbee D, Gavrilov D, Klee EW and Lanpher B: Mitochondrial 3-hydroxy-3-methylglutaryl-CoA synthase deficiency: Unique presenting laboratory values and a review of biochemical and clinical features. JIMD Rep 40: 63-69, 2018.
12. Lee T, Takami Y, Yamada K, Kobayashi H, Hasegawa Y, Sasai H, Otsuka H, Takeshima Y and Fukao T: A Japanese case of mitochondrial 3-hydroxy-3-methylglutaryl-CoA synthase deficiency who presented with severe metabolic acidosis and fatty liver without hypoglycemia. JIMD Rep 48: 19-25, 2019.
13. Morris AA, Lascelles CV, Olpin SE, Lake BD, Leonard JV and Quant PA: Hepatic mitochondrial 3-hydroxy-3-methylglutaryl-coenzyme a synthase deficiency. Pediatr Res 44: 392-396, 1998.
14. Kimura M, Yamamoto T and Yamaguchi S: Automated metabolic profiling and interpretation of GC/MS data for organic acidemia screening: A personal computer-based system. Tohoku J Exp Med 188: 317-334, 1999.
15. Fujiki R, Ikeda M, Yoshida A, Akiko M, Yao Y, Nishimura M, Matsushita K, Ichikawa T, Tanaka T, Morisaki H, *et al*: Assessing the accuracy of variant detection in cost-effective gene panel testing by next-generation sequencing. J Mol Diagn 20: 572-582, 2018.
16. Li H and Durbin R: Fast and accurate short read alignment with burrows-wheeler transform. Bioinformatics 25: 1754-160, 2009.
17. Koboldt DC, Zhang Q, Larson DE, Shen D, McLellan MD, Lin L, Miller CA, Mardis ER, Ding L and Wilson RK: VarScan 2: Somatic mutation and copy number alteration discovery in cancer by exome sequencing. Genome Res 22: 568-576, 2012.
18. McKenna A, Hanna M, Banks E, Sivachenko A, Cibulskis K, Kernytsky A, Garimella K, Altshuler D, Gabriel S, Daly M and DePristo MA: The genome analysis toolkit: A MapReduce framework for analyzing next-generation DNA sequencing data. Genome Res 20: 1297-1303, 2010.
19. Van der Auwera GA, Carneiro MO, Hartl C, Poplin R, Del Angel G, Levy-Moonshine A, Jordan T, Shakir K, Roazen D, Thibault J, *et al*: From FastQ data to high confidence variant calls: The genome analysis toolkit best practices pipeline. Curr Protoc Bioinformatics 43: 11.10.1-11.10.33, 2013.
20. Schwarz JM, Cooper DN, Schuelke M and Seelow D: MutationTaster2: Mutation prediction for the deep-sequencing age. Nat Methods 11: 361-362, 2014.
21. Song XQ, Fukao T, Yamaguchi S, Miyazawa S, Hashimoto T and Orii T: Molecular cloning and nucleotide sequence of complementary DNA for human hepatic cytosolic acetoacetyl-coenzyme A thiolase. Biochem Biophys Res Commun 201: 478-485, 1994.
22. Bradford MM: A rapid and sensitive method for the quantitation of microgram quantities of protein utilizing the principle of protein-dye binding. Anal Biochem 72: 248-254, 1976.
23. Clinkenbeard KD, Reed WD, Mooney RA and Lane MD: Intracellular localization of the 3-hydroxy-3-methylglutaryl coenzme A cycle enzymes in liver. Separate cytoplasmic and mitochondrial 3-hydroxy-3-methylglutaryl coenzyme A generating systems for cholesterogenesis and ketogenesis. J Biol Chem 250: 3108-3116, 1975.
24. Lowe DM and Tubbs PK: 3-Hydroxy-3-methylglutaryl-coenzyme A synthase from ox liver. Properties of its acetyl derivative. Biochem J 227: 601-607, 1985.
25. Rardin MJ, He W, Nishida Y, Newman JC, Carrico C, Danielson SR, Guo A, Gut P, Sahu AK, Li B, *et al*: SIRT5 regulates the mitochondrial lysine succinylome and metabolic networks. Cell Metab 18: 920-933, 2013.
26. Decker K: Acetoacetyl Coenzyme A. In: Methods of enzymatic analysis. 3rd edition, Vol. 7, Metabolites 2: Tri- and dicarboxylic acids, purines, pyrimidines and derivatives, coenzymes, inorganic compounds. Bergmeyer HU, Bergmeyer J and Graßl M (eds.). Wiley-Blackwell, Hoboken, pp201-206, 1985.
27. Aledo R, Zschocke J, Pié J, Mir C, Fiesel S, Mayatepek E, Hoffmann GF, Casals N and Hegardt FG: Genetic basis of mitochondrial HMG-CoA synthase deficiency. Hum Genet 109: 19-23, 2001.
28. Ramos M, Menao S, Arnedo M, Puisac B, Gil-Rodríguez MC, Teresa-Rodrigo ME, Hernández-Marcos M, Pierre G, Ramaswami U, Baquero-Montoya C, *et al*: New case of mitochondrial HMG-CoA synthase deficiency. Functional analysis of eight mutations. Eur J Med Genet 56: 411-415, 2013.
29. Neupert W: Protein import into mitochondria. Annu Rev Biochem 66: 863-917, 1997.
30. Fukao T, Yamaguchi S, Scriver CR, Dunbar G, Wakazono A, Kano M, Orii T and Hashimoto T: Molecular studies of mitochondrial acetoacetyl-coenzyme A thiolase deficiency in the two original families. Hum Mutat 2: 214-220, 1993.
31. Puisac B, Marcos-Alcalde I, Hernandez-Marcos M, Tobajas Morlana P, Levtova A, Schwahn BC, DeLaet C, Lace B, Gómez-Puertas P and Pié J: Human mitochondrial HMG-CoA synthase deficiency: Role of enzyme dimerization surface and characterization of three new patients. Int J Mol Sci 19: 1010, 2018.
32. Kompare M and Rizzo WB: Mitochondrial fatty-acid oxidation disorders. Semin Pediatr Neurol 15: 140-149, 2008.
33. Aledo R, Mir C, Dalton RN, Turner C, Pié J, Hegardt FG, Casals N and Champion MP: Refining the diagnosis of mitochondrial HMG-CoA synthase deficiency. J Inherit Metab Dis 29: 207-211, 2006.
34. Lascelles CV and Quant PA: Investigation of human hepatic mitochondrial 3-hydroxy-3-methylglutaryl-coenzyme A synthase in postmortem or biopsy tissue. Clin Chim Acta 260: 85-96, 1997.
35. Reed WD, Clinkenbeard D and Lane MD: Molecular and catalytic properties of mitochondrial (ketogenic) 3-hydroxy-3-methylglutaryl coenzyme A synthase of liver. J Biol Chem 250: 3117-3123, 1975.
36. Romani AM: Cellular magnesium homeostasis. Arch Biochem Biophys 512: 1-23, 2011.
37. Shafqat N, Turnbull A, Zschocke J, Oppermann U and Yue WW: Crystal structures of human HMG-CoA synthase isoforms provide insights into inherited ketogenesis disorders and inhibitor design. J Mol Biol 398: 497-506, 2010.